

# Measuring How Well a Structure Supports Varying External Wrenches

François Guay<sup>1</sup>, Philippe Cardou<sup>1</sup>, Ana Lucia Cruz Ruiz<sup>2</sup>, and Stéphane Caro<sup>3</sup>

<sup>1</sup> *Laboratoire de robotique, Département de génie mécanique, Université Laval, Quebec City, QC, Canada. e-mail: francois.guay.2@ulaval.ca, pcardou@gmc.ulaval.ca*

<sup>2</sup> *IRCCyN, École Centrale de Nantes, 1 rue de la Noë, 44321, Nantes, France, e-mail: ana-lucia.cruz-ruiz@eleves.ec-nantes.fr*

<sup>3</sup> *CNRS/IRCCyN, 1 rue de la Noë, 44321, Nantes, France, e-mail: stephane.caro@irccyn.ec-nantes.fr*

**Abstract.** An index is introduced, the minimum degree of constraint satisfaction, which quantifies the robustness of the equilibrium of an object with a single scalar. This index is defined under the assumptions that the object is supported by forces of known lines of action and bounded amplitudes, and that the external perturbation forces and moments vary within a known set of possibilities. A method is proposed to compute the minimum degree of constraint satisfaction by resorting to the quickhull algorithm. The method is then applied to two examples chosen for their simplicity and diversity, as evidence of the broad spectrum of applications that can benefit from the index. The first example tackles the issue of fastening a workpiece, and the second, the workspace of a cable-driven parallel robot. From these numerical experiments, the minimum degree of constraint satisfaction proves useful in grasping, cable-driven parallel robots, Gough-Stewart platforms and other applications.

**Key words:** Kinematic index, dexterity, manipulability, kinematic sensitivity, grasping, stability, cable-driven robot, wire-driven robot, Gough-Stewart platform.

## 1 Introduction

In mechanism and structure design, the definition of a sound and meaningful performance index that would apply to a wide variety of situations would be of tremendous help. Such a concept would allow the automation of a part of the design process, enabling a systematic scan of the possible solutions. With this objective in mind, several researchers have proposed indices—see the excellent review by Merlet [5].

Among the most popular indices, we find the *manipulability*, originally proposed by Yoshikawa [9]. This index represents the volume of the ellipsoid obtained by mapping the unit-sphere through the Jacobian matrix of a robotic manipulator. Hence, the manipulability represents a geometric average of the kinematic sensitivity of the robot. If the kinematic sensitivity is null in one direction of motion, then the ellipsoid becomes flat, and its volume zero. This implies that the robot cannot support an object in this direction of motion. The drawback of this approach is that a manipulator may be very close to instability while retaining a large manipulability if its associated ellipsoid is thin along one dimension and thick along the others.

Another widely used index is the *dexterity*, as defined by Salisbury and Craig [7]. Geometrically, this index measures the distortion of the ellipsoid associated with the Jacobian matrix of a manipulator by taking the ratio of its largest semi-axis to its smallest. The problem with this approach is that it does not account for the size of the ellipsoid. Thus, the concept of capacity is occluded by that of evenness.

Another drawback of dexterity is that it is ill-defined when the Jacobian matrix is not dimensionally-homogeneous, a problem that has been noted by several authors. Workarounds have been proposed [1, 8, 4], but all of them entail some arbitrariness, and, perhaps for this reason, have not generally received acceptance from the robotics community. In this paper, we propose a normalisation that is no less arbitrary than those proposed previously, but that has the merit of being simple and straightforward. In any case, as was pointed out by Park and Kim [6], “arbitrariness is an unavoidable consequence of the geometry of  $SE(3)$ .”

Most importantly, the dexterity and the manipulability do not account for the varying force and moment capabilities of the actuators, nor for the external forces and moments that the object has to support. In general, the designer can and must evaluate these constraints during the design process.

In this paper, we take into account the actuator capacities, as well as the set of expected external forces and moments, and incorporate them into the definition of our performance index. These assumptions are formally explained in section 2. In section 3, we define the proposed index, various examples of increasing complexities are presented in sections 4 and 5, and a summary is given in section 6.

## 2 Mechanical Model of a Structure Supporting an Object

We start from a rigid body in space, whose free-body diagram is shown in Fig. 1. This object is subjected to a system of external forces (e.g., gravity or air friction), which we represent by their resulting force at  $E$  and moment,  $\mathbf{f}_e$  and  $\mathbf{n}_e$ . The location of point  $E$  generally depends on the application considered, and experience shows that the choice of  $E$  is usually straightforward. The external wrench is to be balanced by the forces  $\mathbf{f}_i$ ,  $i = 1, \dots, m$ , applied by the supporting structure on the object at the corresponding points  $C_i$ ,  $i = 1, \dots, m$ . We assume that the directions of these forces are known and given by unit vectors  $\mathbf{u}_i$ ,  $i = 1, \dots, m$ . When the supporting forces come from physical contacts between the object and the structure, this implies the absence of friction, and vectors  $\mathbf{u}_i$  pointing towards the object. When the object is suspended by a cable, then  $\mathbf{u}_i$  points in the direction opposite to the object.

From Fig. 1, the equations of static equilibrium are

$$\mathbf{W}\mathbf{f} + \mathbf{w}_e = \mathbf{0}_6, \quad (1)$$

where

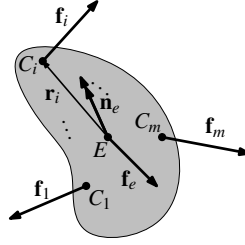


**Fig. 1** Free-body diagram of an object in space

$$\mathbf{W} \equiv \begin{bmatrix} \mathbf{u}_1 & \cdots & \mathbf{u}_m \\ \frac{1}{r}\mathbf{r}_1 \times \mathbf{u}_1 & \cdots & \frac{1}{r}\mathbf{r}_m \times \mathbf{u}_m \end{bmatrix}, \mathbf{f} \equiv \begin{bmatrix} f_1 \\ \vdots \\ f_m \end{bmatrix}, \mathbf{w}_e \equiv \begin{bmatrix} \mathbf{f}_e \\ (1/r)\mathbf{n}_e \end{bmatrix},$$

$f_i$  is the amplitude of the  $i^{\text{th}}$  force,  $\mathbf{0}_3$  is the three-dimensional zero vector, and  $r^2 = (1/m) \sum_{i=1}^m \|\mathbf{r}_i\|_2^2$  is used to render the equations dimensionally homogeneous. One may see a problem occurring when  $r = 0$  m, that is when all points  $C_i$ ,  $i = 1, \dots, m$ , are located at  $E$ . In such a case, all forces are concurrent at  $E$ , so that the rigid body becomes a particle, and a sum of moments is no longer needed.

We assume that the external wrenches  $\mathbf{w}_e$  that could be applied on the object by its environment form a known polytope, the set of task wrenches  $\mathcal{T}$ , or

$$\mathcal{T} = \{\mathbf{w}_e \in \mathbb{R}^6 : \mathbf{w}_e = \sum_{j=1}^n \alpha_j \mathbf{w}_{e,j}, \sum_{j=1}^n \alpha_j = 1, \alpha_j \geq 0, j = 1, \dots, n\}. \quad (2)$$

The designer generally has an approximate idea of the wrenches that will be applied by the environment, which he or she can approximate with the polytope  $\mathcal{T}$ .

We also work under the assumption that the structure can only withstand forces  $f_i$  within given ranges, e.g., the limited resistance of the contact surface, the inability of cables to push, or the limited capacities of actuators. These ranges of forces form the set  $\mathcal{F}$  of feasible forces, a box (a.k.a. orthotope) in  $m$ -dimensional space, namely,

$$\mathcal{F} = \{\mathbf{f} \in \mathbb{R}^m : \underline{\mathbf{f}} \leq \mathbf{f} \leq \bar{\mathbf{f}}\}, \quad (3)$$

where  $\underline{\mathbf{f}}$  and  $\bar{\mathbf{f}}$  are the lower and upper bounds on the force array  $\mathbf{f}$ .

### 3 A Measure of the Structure Capacity

For the object to remain in equilibrium, it must not only satisfy the static equilibrium equations (1), but also have supporting forces  $\mathbf{f}$  within the allowed ranges for any of the task wrenches  $\mathbf{w}_e$ . These conditions can be symbolically expressed as

$$\forall \mathbf{w} \in \mathcal{T}, \exists \mathbf{f} \in \mathcal{F} : \mathbf{w}_e = -\mathbf{W}\mathbf{f}. \quad (4)$$

This condition can also be understood graphically. The two sets  $\mathcal{F}$  and  $\mathcal{T}$  are defined in different spaces, which are connected through the linear relationship of the equation of static equilibrium. In Fig. 2, the box  $\mathcal{F}$  of allowed forces is mapped onto the wrench space through the linear transformation  $\mathbf{w} = -\mathbf{W}\mathbf{f}$ . The resulting set is labelled  $\mathcal{W}$ , and is a special type of polytope called a zonotope [2]. From the feasibility condition (4), we conclude that the system is in equilibrium if and only if

$$\mathcal{T} \subseteq \mathcal{W}. \quad (5)$$

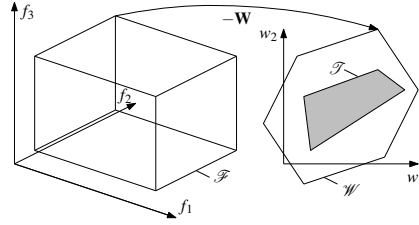


**Fig. 2** An analog representation of the mapping of  $\mathcal{F}$  onto the wrench space

Our measure should be a function indicating how far set  $\mathcal{T}$  is from being partly outside of  $\mathcal{W}$ . It should be positive when the structure can support the task wrenches, and negative otherwise. It should be as smooth as possible to ease its optimisation.

As an indicator of the *degree of inclusion* of  $\mathcal{T}$  within  $\mathcal{W}$ , we propose an index that we call the *minimum degree of constraint satisfaction*, and which we define as

$$s = \min_{j=1,\dots,n} \left( \min_{l=1,\dots,p} s_{j,l} \right), \quad (6)$$

where the degree of constraint satisfaction  $s_{j,l}$  is the signed distance from vertex  $\mathbf{w}_{e,j}$  of  $\mathcal{T}$  to the  $l^{\text{th}}$  face of  $\mathcal{W}$ . We take  $s_{j,l}$  to be positive when the constraint is satisfied, and negative otherwise. With this definition, the minimum degree of constraint satisfaction  $s$  remains negative as long as at least one of the vertices of  $\mathcal{T}$  remains outside of  $\mathcal{W}$ ; becomes zero whenever  $\mathcal{T} \subseteq \mathcal{W}$  and a vertex of  $\mathcal{T}$  lies on the boundary of  $\mathcal{W}$ ; and is positive when  $\mathcal{T}$  is in the interior of  $\mathcal{W}$ .

The computation of the proposed indicator function is performed in five steps:

(i) Compute the vertices of  $\mathcal{F}$ ,  $\mathbf{f}_k$ ,  $k = 1, \dots, q$ ,  $q = 2^m$ , through the formula  $\mathbf{f}_k = (\mathbf{1}_{m \times m} - \text{diag}(\beta_k))\underline{\mathbf{f}} + \text{diag}(\beta_k)\bar{\mathbf{f}}$ , where  $\beta_k$  is the array of  $m$  bits giving the binary representation of  $k$ .

(ii) Map the vertices onto the wrench space as  $\mathbf{w}_k = -\mathbf{W}\mathbf{f}_k$ ,  $k = 1, \dots, q$ .

(iii) Compute the convex hull of  $\mathcal{W}$  from  $\mathbf{w}_k$ ,  $k = 1, \dots, q$ . Fortunately, several routines are readily-available for this purpose. Here, we use the quickhull algorithm implemented in the `qhull` package for Matlab. This returns the polytope  $\mathcal{W}$  in the form  $\mathcal{W} = \{\mathbf{w} \in \mathbb{R}^6 : \mathbf{a}_l^T \mathbf{w} \leq b_l, l = 1, \dots, p\}$ .

(iv) Compute the degree of constraint satisfaction  $s_{j,l}$  associated with the  $j^{\text{th}}$  vertex of  $\mathcal{T}$ ,  $\mathbf{w}_{e,j}$ , and the  $l^{\text{th}}$  face of  $\mathcal{W}$ ,  $\mathbf{a}_l^T \mathbf{w} = b_l$ . This is done by projecting a vector from  $\mathbf{w}_{e,j}$  to the hyperplane of the  $l^{\text{th}}$  face of  $\mathcal{W}$  onto its normal  $\mathbf{a}_l / \|\mathbf{a}_l\|_2$ , which gives  $s_{j,l} = (b_l - \mathbf{w}_{e,j}^T \mathbf{a}_l) / \|\mathbf{a}_l\|_2$ .

(v) Compute the *closeness* of  $\mathcal{T}$  to being completely included in  $\mathcal{W}$  as the minimum  $s$  of the degrees of constraint satisfaction, as per eq. (6).

#### 4 Example: Holding a Workpiece

In this example, we consider the problem of clamping a metal block having dimensions 150 mm  $\times$  100 mm for a polishing run. The polisher consists of a rotating circular brush following a strip pattern, applying a moment of 500 N-mm, and a force of 100 N in the direction of the brush motion. We are to determine the optimal four-contact-point pattern that provides the most robust equilibrium.

A free-body diagram of our metal block is shown in Fig. 3. We assume that each contact point is on a distinct edge of the rectangle and that friction is negligible. We parameterise the positions of the forces  $f_1$  and  $f_2$  with  $x$  and  $y$  and assume that the remaining forces are symmetric to  $f_1$  and  $f_2$  with respect to the origin.

The weight of the metal block is ignored, so that the task wrench set  $\mathcal{T}$  is solely determined by the forces and moments applied by the tool. The force-moment system  $(\mathbf{f}_e, n_e)$  equivalent to each possible position and direction of motion of the brush is computed as  $\mathcal{T} = \{\mathbf{f}_e \in \mathbb{R}^2, n_e \in \mathbb{R} : \|\mathbf{f}_e\|_\infty \leq 100 \text{ N}, |n_e| \leq 15 \text{ N m}\}$ .

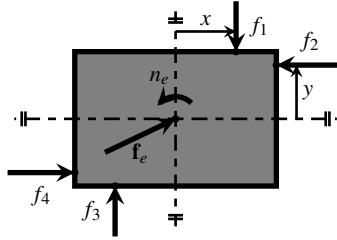
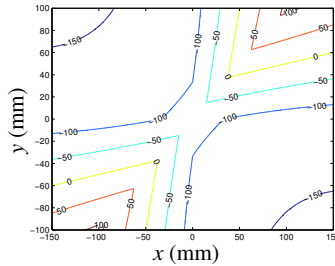


Fig. 3 Free-body diagram of the workpiece

The minimum degree of constraint satisfaction  $s$  is computed for all possible positions of  $f_1$  and  $f_2$ , which results in the graph of Fig. 4. In this figure, recall that the  $x$ -axis represents the positions of  $f_1$  on the upper edge, while the  $y$ -axis represents that of  $f_2$  on the right edge. Figure 4 shows that the metal block is best held in place by choosing the contact points at  $x = 100$  mm and  $y = 95$  mm. Interestingly, the contour  $s = 0$  N corresponds to the stability frontier, so that we must have  $|x| \geq 40$  mm and  $|y| \geq 40$  mm for the workpiece to be stable.



**Fig. 4** Isocontours of the proposed index  $s$  in Newtons as a function of the contact-point positions

## 5 Example: The Wrench-Feasible Workspace (WFW) of a Planar Cable-Driven Parallel Robot (CDPR)

Let us use the index  $s$  to trace the WFW of a cable-driven parallel robot CDPR. A cable-driven parallel robot is a parallel robot that utilizes cables instead of rigid links. This particular characteristic provides CDPRs with advantages such as high dynamics and a large workspace, however their workspace is greatly reduced by the fact that eq. (4) can only be satisfied with non-negative forces or feasible cable tensions (the cables can pull but not push).

For such robots, the set of feasible forces  $\mathcal{F}$  defined in eq. (3) becomes the set of feasible cable tensions. The sets  $\mathcal{W}$  and  $\mathcal{T}$  in Fig. 2 define the available and required wrench sets of the robot. The available wrench set represents the ability of the cables to generate forces and moments on the moving platform, while the required wrench set represents the forces and moments that are applied by the environment on the platform for a specific task.

The WFW is the set of mobile platform poses for which the required wrench set is contained in the available wrench set. This implies that a pose belonging to the WFW must satisfy eq. (5) and that the tensions along each cable should be non-negative and respect a tension range subject to the capabilities of the actuators. This workspace can be traced along a given area by using the minimum degree of constraint satisfaction to measure the degree of inclusion of the required wrench set polytope in the available wrench set polytope for each pose. The condition  $s = 0$  defines the stability frontier, that is, the boundary of the WFW of the CDPR, and the positive values of  $s$  correspond to poses inside the WFW.

We used this observation to revisit the example of Fig. 5 of Gouttefarde et al. [3]. In this example, the geometry of the CDPR is as illustrated in Fig. 5,  $\mathcal{F} = \{\mathbf{f} \in \mathbb{R}^4 : \|\mathbf{f}\|_\infty \leq 50 \text{ N}\}$ , and  $\mathcal{T} = \{\mathbf{f}_e \in \mathbb{R}^2, n_e \in \mathbb{R} : \|\mathbf{f}_e\|_\infty \leq 10 \text{ N}, |n_e| \leq 0.5 \text{ Nm}\}$ . We compute the minimum degree of constraint satisfaction  $s$  for each pose along a three dimensional grid. The robot is displaced along the XY plane and rotated through a range of orientations from  $-36^\circ$  to  $36^\circ$ . The top and 3D views of the resulting WFW are shown in Fig. 5, and correspond to those obtained in [3]. The computed surface defines the stability frontier, therefore the platform must be kept within this boundary in order to remain stable.

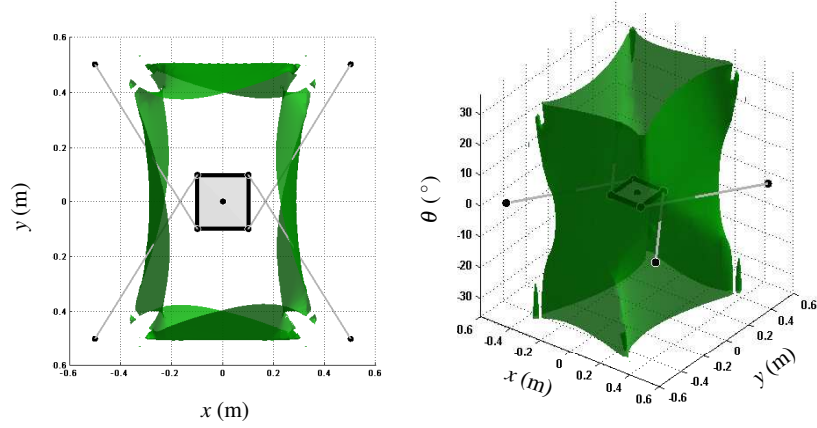


**Fig. 5** Boundary of the total-orientation WFW for the example proposed by Gouttefarde et al. [3]

In order to obtain a more quantitative view of the capacity of the robot to withstand the required wrench set, the minimum degree of constraint satisfaction was also used to compute the constant orientation WFW. Figure 6 shows the resulting workspaces for fixed orientations of  $0^\circ$  and  $45^\circ$ , which also correspond to those obtained in [3]. The contour where  $s = 0$  defines the stability frontier. We note that the workspace is contained inside the convex hull formed by the base anchor points and that its shape and size are altered by the  $45^\circ$  rotation of the platform. We also note that in both cases the CDPR has a higher capacity to balance the required wrench set at the center of the workspace, and that this capacity is gradually reduced as the platform is shifted away from the center.

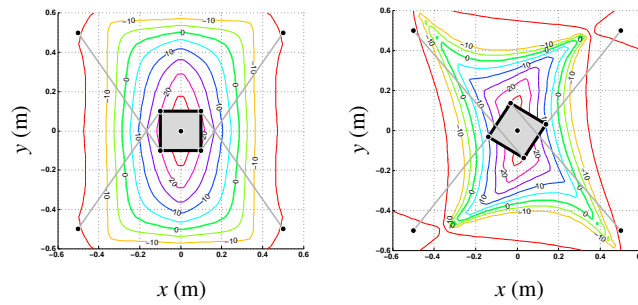


**Fig. 6** Isocontours of the proposed index  $s$  in Newtons as a function of the pose

## 6 Conclusions

In summary, we have defined a new kinetostatic index that is quite general, as demonstrated by the variety of the presented examples. In short, this index informs the designer of the closeness to instability, in Newtons. A negative value of the index indicates an unstable design, and a positive value, a stable one. We believe the index to be an interesting alternative to the manipulability and the dexterity, as it takes into account not only the geometry of the device, but also the forces and moments required by the task or allowed by the actuators or support members. Moreover, the minimum degree of constraint satisfaction represents the worst-case scenario, unlike manipulability and dexterity, which is thought more useful to the designer. The index is not flawless, however, and we are currently exploring alternative solutions to the dimensional homogeneity problem and to the associated computational burden.

## References

1. Angeles, J.: The design of isotropic manipulator architectures in the presence of redundancies. *The International Journal of Robotics Research* **11**(3), 196–201 (1992)
2. Bouchard, S., Gosselin, C., Moore, B.: On the ability of a cable-driven robot to generate a prescribed set of wrenches. *ASME Journal of Mechanisms and Robotics* **2**(1), 011,010 (2010)
3. Gouttefarde, M., Daney, D., Merlet, J.P.: Interval-analysis-based determination of the wrench-feasible workspace of parallel cable-driven robots. *IEEE Transactions on Robotics* **27**(1), 1–13 (2011)
4. Khan, W.A., Angeles, J.: The kinetostatic optimization of robotic manipulators: The inverse and the direct problems. *ASME Journal of Mechanical Design* **128**(1), 168–178 (2006)
5. Merlet, J.P.: Jacobian, manipulability, condition number, and accuracy of parallel robots. *ASME Journal of Mechanical Design* **128**(1), 199–206 (2006)
6. Park, M.K., Kim, J.W.: Kinematic manipulability of closed chains. In: *Advances in Robot Kinematics*, pp. 99–108. Portoroz-Bernadin (1996)
7. Salisbury, J.K., Craig, J.J.: Articulated hands: Force control and kinematic issues. *The International Journal of Robotics Research* **1**(4), 4–17 (1982)
8. Tandirci, M., Angeles, J., Farzam, R.: Characteristic point and the characteristic length of robotic manipulators. In: *ASME Design Engineering Conferences, 22nd Biennial Mechanisms Conference* (1992)
9. Yoshikawa, T.: Analysis and control of robot manipulators with redundancy. In: *Proceedings of the First International Symposium on Robotics Research*, pp. 735–747. Bretton Woods, NH, USA (1983)